Annu. Rev. Earth Planet. Sci. 2004. 32:91–109
doi: 10.1146/annurev.earth.32.071603.152635
Copyright © 2004 by Annual Reviews. All rights reserved

RECENT DEVELOPMENTS IN THE STUDY OF OCEAN TURBULENCE

S.A. Thorpe
Bodfryn, Glanrafon, Llangoed, Anglesey, LL58 8PH, United Kingdom;
email: oss413@sos.bangor.ac.uk

Key Words mixing, surface boundary layer, abyssal ocean, shelf seas

■ **Abstract** This review describes the changes in the understanding of turbulence and mixing in the upper layers of the ocean, the abyssal ocean, and in continental shelf seas that have come in the past 25 years, largely through advances in instruments and methodology.

1. INTRODUCTION

Ocean turbulence was reviewed by Gargett in 1989. Although not intended to be comprehensive, her critical account of the subject elegantly covered much of what was known at that time. The purpose of this review is to describe the background and history of some of the developments which, in my view, are the most striking and significant to have taken place since then.

The subject of ocean turbulence has attained a greater degree of importance, and the focus of attention has altered for two main reasons, each related to prediction. The growing densities of population in cities and towns adjoining the coastal seas, with accompanying growth in fishing, discharges, and recreational use of the seas, have imposed greater stress on the marine environment and enhanced the requirement for better management. Turbulence helps to disperse pollutants and exerts strong controls on the growth and vitality of marine organisms, especially those at the foot of the food web, the plankton, and further knowledge is central to improved predictive modeling. There is also the enhanced need to model climate change. It is now recognized that small-scale turbulent diffusion in the depths of the ocean affects the overall ocean circulation. Transfers of momentum, heat, and gases across and near the ocean surface, and the turbulent motions within the relatively uniform mixed layer of the ocean, are largely controlled by waves, especially breaking waves. Ocean circulation, air-sea transfers, and plankton abundance have substantial effects on climate. The understanding of how turbulence is produced and its nature and effects in shallow seas, the deep ocean, and in the mixed layer is consequently of considerable importance and practical application.

Gargett's review (limited, as is this, by space) includes the following main headings: Surface Boundary Layer, Mixing in the Stratified Interior (including double-diffusion and shear-generated turbulence), and Diapycnal Mixing in Ocean Models. Effects of topography are scarcely referred to, and tides are not mentioned at all. In view of recent changes in emphasis (and because of personal interests—my "ocean" differs somewhat from that selected by Gargett), my topics are slightly different. Her first two general topics remain of paramount importance and are therefore included in this review in Sections 3 and 4, but I omit double-diffusive processes [not that they are unimportant—the interested reader should see St Laurent & Schmitt (1999)] and I "broaden the ocean" to include reference in Section 5 to regions confined by topography, the shallow seas of the continental shelves, and straits. There are cautionary lessons to be learned in the latter.

Although mesoscale motions of 100 km scale have characteristics of turbulence and play a key role, along with the processes associated with planetary waves, in the dispersion of momentum, heat, and matter dissolved in the ocean (e.g., see Thorpe 1998), attention here is mainly confined to those processes leading to turbulence at scales of order 1 mm to 100 m in which the Earth's rotation and curvature have little or no immediate effect. Figure 1 is a cartoon illustrating some of the features referred to below. The focus is on measurements rather than theory because novel developments in measurement have led the way in advancing knowledge and illustrate the severe challenges and meticulous care required in quantifying small-scale turbulent processes. The consequences of new measurements for ocean modeling are not described in detail in spite of the importance of forecasting the future or understanding the past ocean circulation or the climate.

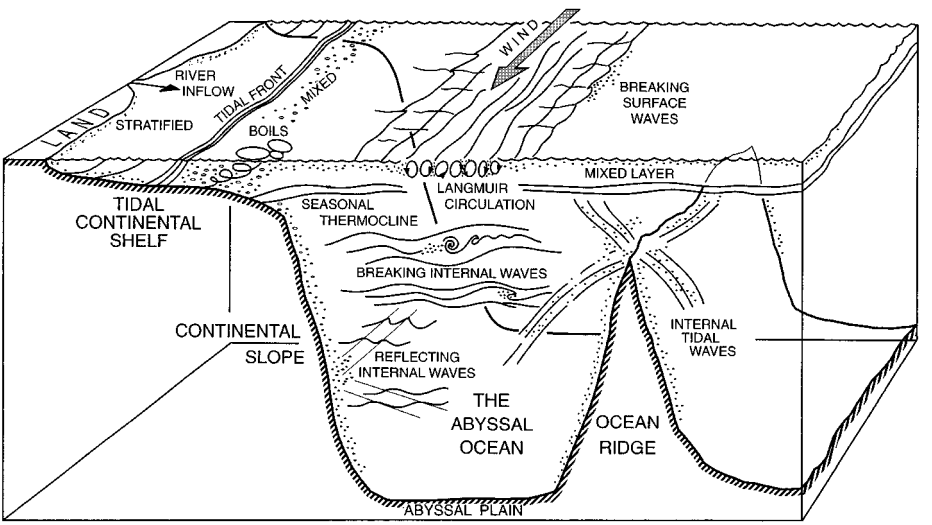

Figure 1 Sketch (not to scale) showing some of the features mentioned in text that are related to ocean turbulence. Regions of strong turbulence are stippled.

Where appropriate, references are given to guide those wishing to probe more deeply into the subject. Recent publications by Kantha & Clayson (2000a,b) and Baumert et al. (2004) provide comprehensive texts about small-scale turbulent processes in the ocean and of ocean models.

2. TURBULENCE AND ITS MEASUREMENT

No precise, robust, and fully transparent or clear definition of what is meant by turbulence has been devised. Turbulence is generally accepted to be an energetic, rotational, and eddying state of motion that disperses material and transforms momentum at rates far higher than those of molecular processes alone. Perhaps its most important property, and one which is generally used to characterize it, is that by generating relatively large gradients of velocity at small scales, typically 1 mm to 1 cm, turbulence promotes viscous dissipation that transfers its kinetic energy into heat. In the ocean, this heating is dynamically insignificant (the resulting changes in buoyancy are generally minute), but the loss of energy is substantial and fundamental to the working of the ocean. Turbulence is conventionally quantified by the rate of loss of the kinetic energy of the turbulent motion per unit mass, usually denoted by ε. Its units are $m^2\ s^{-3}$ or equivalently Wkg^{-1}. Typical values range from $10^{-10}\ m^2\ s^{-3}$ in the abyssal ocean (Toole et al. 1994) to $10^{-1}\ m^2\ s^{-3}$ in the most active regions, in rapid tidal currents, and in the surf zone. Enhanced gradients of temperature or dissolved solutes (e.g., salt) produced by the straining of their respective fields by turbulent eddies result in relatively rapid diffusion at a molecular scale, "turbulent diffusion," as opposed to a tendency of turbulent eddies to engulf surrounding fluid and spread material or dissolved substances by "turbulent dispersion."

Direct measurement of the dissipation rate, ε, is not possible, but estimates can be obtained by means of air-foil shear probes devised by Osborn (1974). These consist of a piezoelectric crystal, similar to those once used in gramophone pick-ups, protected by a rubber sheath with a diameter of approximately 5 mm. These delicate probes are mounted, exposed to the relative oncoming flow, on a stable, largely vibration-free "platform." Various platforms have been used: free-fall[1] or moored instruments (Lueck et al. 1997); submarines (Osborn et al. 1992); and automated underwater vehicles (AUV) (Thorpe et al. 2003a), moving steadily

[1]A free-fall instrument is one that is released from a ship at the sea surface to fall through the water, recording data on a vertical profile. Turbulence probes are mounted at the bottom of the instrument, exposed to undisturbed water. Great care is needed to avoid self-induced vibrations that may effect turbulence measurements. Return to the surface for recovery is either by releasing a weight or through a very light-weight and flexible tether, usually with fiber optic cable to transmit data back in real time. Examples are the Advanced Microstructure Profiler, AMP, devised by Gregg (Gregg et al. 1986), the fine and microstructure profiler, HRP (Schmitt et al. 1988), and the Fast Light Yoyo, FLY, system used in shallow waters (Dewey et al. 1987).

through the water at speeds usually about 0.5–2 ms^{-1}. The probes provide electrical signals proportional to the changes in lateral force, which can be calibrated to give the rate of change of the relative lateral speed of the water, the shear, at frequencies greater than 200 Hz. With certain severe assumptions about the isotropy of the turbulent motion and the form of the spectrum of turbulence (e.g., see Gregg et al. 1986, Gregg 1999), these can be converted into estimates of ε, usually averaged over approximately one-second intervals, but commonly with uncertainty in the estimates of 50%. This may appear large, but because ε generally ranges over many decades, it is often less important than first appears.

I shall refer to other, even less direct, ways of estimating ε in sections below. Descriptions of several other methods of measuring turbulence are given in the *Journal of Atmospheric and Oceanic Technology*, volume 16, pp. 1465–667, dedicated to Dr. R.W. Stewart, an early and distinguished leader in the field.

3. NEAR-SURFACE TURBULENCE

Only in recent years have substantial advances been made in investigating turbulence just below the sea surface. Flow close to fixed boundaries has long been of interest in the design of aircraft wings and in the understanding of the transport of sediment near the seabed. The flow exerts a stress, τ, on the boundary, which can be expressed in terms of a friction velocity, u_*, and water density, ρ, as $\tau = \rho u_*^2$. At distances, z, from a rigid boundary, the dissipation rate generally follows the Law of the Wall relation, $\varepsilon = u_*^3/kz$, where k is von Karmàn's constant, approximately 0.41. At depths below the sea surface greater than approximately the significant wave height (the mean height of the highest 1/3 of the waves), Hs, the dissipation rate, ε, also follows the Law of the Wall, with u_* given by the wind stress on the sea surface, τ_w.[2] In the early 1990s, it became clear that values of ε closer to the sea surface than Hs were higher than those of the Law of the Wall relationship because of the turbulence generated by breaking waves (Agrawal et al. 1992) (see Figure 2).

Accurate measurements in this near-surface region are hard because of the sometimes-violent motions caused by waves, and untangling the turbulent motion from those induced by waves is difficult. Advances came mainly from two complementary sources: laboratory experiments and field observations (particularly in lakes). In laboratory experiments, Rapp & Melville (1990) demonstrated that breaking involves the loss of approximately 10% of a wave's energy in spilling breakers and as much as 25% in plunging breakers. Approximately 90% of the energy lost by a wave in breaking is dissipated by turbulence within a time of four

[2]The measurement of τ_w is no easy matter, but it can be related to the square of the wind speed, W, via a drag coefficient, C_D: $\tau = \rho_a C_D W^2$, where ρ_a is the density of air, approximately $1.2 \times 10^{-3}\ \rho$. C_D is typically (1–2.5) $\times\ 10^{-3}$, but increases with W; see Jones & Toba (2001).

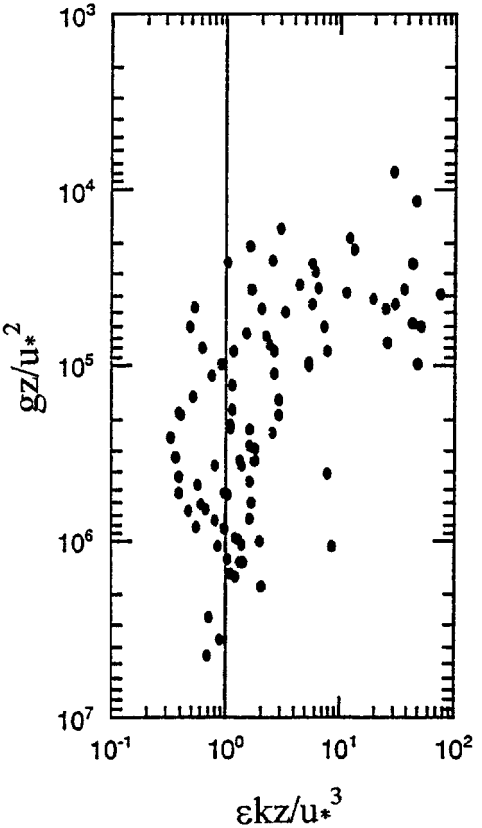

Figure 2 The observed variation of the rate of loss of turbulent kinetic energy, ε, with depth, z, below the sea surface. The coordinates are scaled according to the Law of the Wall so that points near the surface ($gz/u_*^2 < 10^5$) to the right of the vertical line at $\varepsilon kz/u_*^3 = 1$ are values of ε that exceed the Law values. (From Agrawal et al. 1992.)

wave periods after wave breaking, but some energy is transferred into the formation of a coherent "rotor" or "roller" structure of height comparable to that of the breaking wave, which is left within the water after breaking (Melville et al. 2002). Other subsurface coherent structures in the turbulence generated by breakers are indicated by the patterns observed in the breakup of foam left floating on the water surface after a wave has broken (Thorpe et al. 1999). Radiometer observations show that breakers disrupt the cool thermal boundary layer, approximately 1 mm thick, on the surface of the ocean (Jessop et al. 1997) and consequently affect air-sea heat and gas fluxes (Figure 3).

Terray et al. (1996) propose a parametrization of the energy loss by breakers, or equivalently, of the production of energy within the upper ocean, using the

wave age (the ratio of the phase speed of the dominant waves to the friction velocity, u_*), but careful observations of breaker frequency and speed by Gemmrich & Farmer (1999) suggest that formulation may need to be more sophisticated, depending on the local rate of input of energy from the wind to the wave field. (Swell arriving from distant sources may also play a part.) Duncan (1981) finds that the energy dissipation from breakers per unit crest length depends on the fifth power of their phase speed, c, and is consequently very sensitive to the size of c and to the crest length of breakers. Air-borne photographic measurements of breakers made by Melville & Matusov (2002) show that the distribution of the mean crest length of breakers is proportional to the cube of the wind speed and determine how the length is related to the speed of the breakers. The fraction of the ocean surface mixed by breakers is dominated by relatively slow-moving and short breaking waves. More measurements of turbulence in and immediately after wave breaking at sea are needed, and advancing knowledge of the connection of waves and turbulence should be a high priority for research in coming years.

Large-scale coherent flow structures are found in the turbulent mixed layer. Langmuir (1938) was the first to recognize the dynamical significance of the accumulation of flotsam in so-called windrows on the sea surface aligned parallel to the wind. These bands, often composed of foam, are typically 2–300 m apart, and some are 3–10 times greater in length. What is now known as Langmuir circulation (Leibovich 1983, Thorpe 2004) consists of a set of downwind-directed vortical motions, leading to windrows in convergence lines on the water surface and down-going flows, typically 1–20 cm s^{-1}, beneath, replenished by a broader weaker upward flow between the convergence lines. Langmuir circulation appears to be generated as a result of a vortex force associated with the wave-induced Stokes drift (the so-called CL2 mechanism). It therefore has no immediate analogue in the atmosphere. Buoyant algae, and bubbles generated by breakers and detectable using sidescan sonar, accumulate in the downward flow partly owing to the trapping mechanism described by Stommel (1949) in which the tendency of buoyant particles to rise is countered by the downward flow. Turbulent dissipation rates are also found to be higher than average within the down-going water below windrows (Figure 4), probably owing to a combination of advection into the region of decaying turbulence produced by breaking waves and the shear and stretching of small-scale eddies by the circulation. This localized enhancement of turbulence where algae and bubbles are concentrated has possible consequences for algae dynamics and for gas exchange (Thorpe et al. 2003b). Turbulence affects predator-prey contact and algal fixation rates and may damage flagella or disrupt chain phytoplankton and algal assemblages or flocs. It may reduce bubble rise speeds, cause bubble disruption or enhance coalescence of one bubble with another, and change the dissolution or diffusion rates of gases from bubbles into the water, a pathway for air-sea gas transfer.

The vortical motions of Langmuir circulation are now known to be unsteady and irregular. The bands are convoluted, meander, vacillate in strength, and join

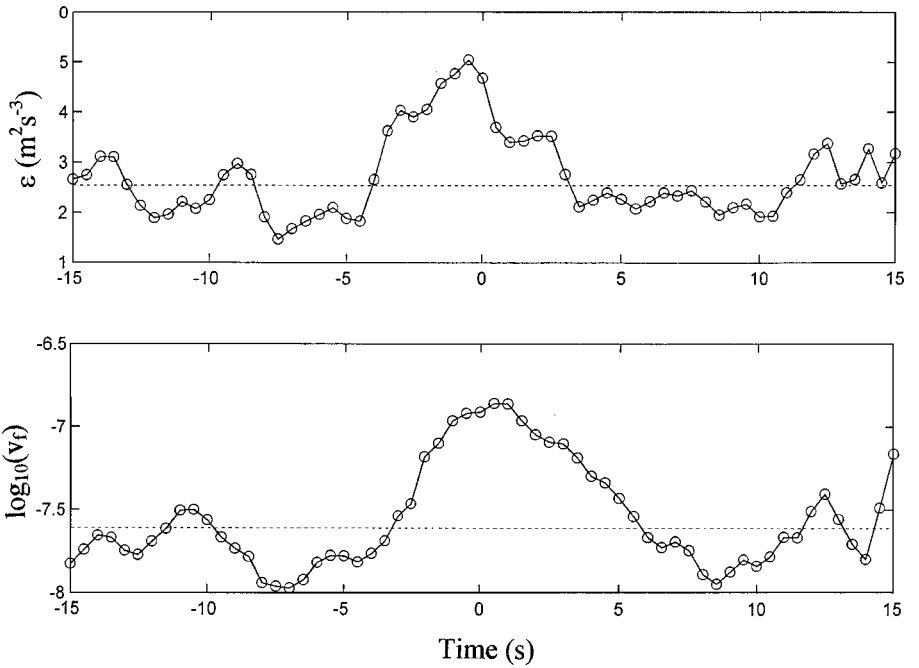

Figure 4 Increased dissipation rates in Langmuir bands. Conditional sample plots averaged across 31 Langmuir bands at time t = 0 and at a depth of 2.1 m (z/Hs = 1.92) in a wind speed of 10.6 m s^{-1} showing the variation of (*top*) $\log_{10}$ of the mean dissipation, ε, and (*below*) $\log_{10}$ of the mean bubble void fraction, v_f, across the bands. (From Thorpe et al. 2003b.)

together. Separations vary, with a hierarchy of simultaneously occurring scales. Langmuir circulation is now regarded as one of the turbulent processes active in the upper ocean (McWilliams et al. 1997). Although it produces local concentrations of floating material in windrows (for example, of oil accidentally spilled on the sea surface), the turbulent characteristics of the bands lead to the spread of pollutants on the water surface. The circulation also contributes substantially to maintaining the vertical uniformity of the upper part of the mixed layer and, by engulfing or entraining water from the underlying thermocline, to early stages of its deepening.

Other large-scale flow structures are detected in the mixed layer. Notable are those resulting from shear that generates coherent eddies that strain the (often very small) mean temperature gradients and lead to "temperature ramps" or "microfronts" (Thorpe 1995). Coherent flow structures, about which less is known, are those driven by convection when the surface loses heat rapidly (see Shay & Gregg 1986).

4. MIXING IN THE ABYSSAL OCEAN

Turbulence near the sea surface is physically accessible but presents measurement challenges that, largely because of wave motion, have yet to be fully overcome. In contrast, the abyssal ocean offers the challenge of inaccessibility, huge pressure, and often patchy and relatively weak turbulence with small dissipation rates.

An early clue to the magnitude of the effects and the processes involved in deep-ocean mixing came from a simple advective-diffusion balance calculation. By comparing transport terms in the heat balance equation, specifically equating the heat carried by upward-going cold water originally formed by cooling in polar regions to the heat transfer by downward mixing of warmer water from the surface in low and mid latitudes, and making the assumption that the temperature is steady, Munk (1966) concluded that the average vertical[3] diffusion coefficient of heat, K_v, at depths below approximately 1500 m is $\sim 10^{-4}$ m^2 s^{-3}. This is a value far greater than the molecular diffusivity of heat, κ, of $\sim 1.4 \times 10^{-7}$ m^{2}s^{-1}, implying that turbulence must be active in transferring heat. The hunt was on to identify the processes responsible!

One of Munk's proposals, and that which appeared most likely, is that the downward heat flux is largely caused by the breaking of internal waves. Internal waves and their breaking is a complex subject that has recently been reviewed by Staquet & Sommeria (2002). In brief, internal waves propagate through the density-stratified ocean, carrying energy from their generation source to deeper or shallower regions. They break, producing mixing and vertical diffusion and dissipating energy, either by steepening and overturning density layers in a manner similar to breaking surface waves or, more likely, through their local enhancement of shear, which leads to an instability called Kelvin-Helmholtz instability in which small undulations grow at a length scale smaller than the waves themselves. Turbulence is reached via a transition that involves a series of stages in which wave-like undulations "roll-up," overturning the density field in "billows" where the fluid becomes statically unstable and small-scale vortical motions occur. (An example of billows detected acoustically is shown in Figure 5.) Considerable effort was put into discovering the form and spectra of internal waves so as to quantify their effect on diffusion. Estimates of K_v from this knowledge are still rather uncertain, but significantly less than Munk's canonical estimate of 10^{-4} m^2 s^{-1}.

Munk's analysis prompted the development of the means to estimate K_v. Three important relationships useful in measurement and vital to relating turbulence, microstructure, and mixing were discovered in the 1970s, and these allowed estimates of turbulent diffusion to be obtained from free-fall microstructure instruments. The

[3]Strictly, K_v should be the diapycnal (meaning across surfaces of constant density) diffusivity coefficient, and care is required in measurement and models to separate diapycnal mixing from the isopycnal mixing along density surfaces.

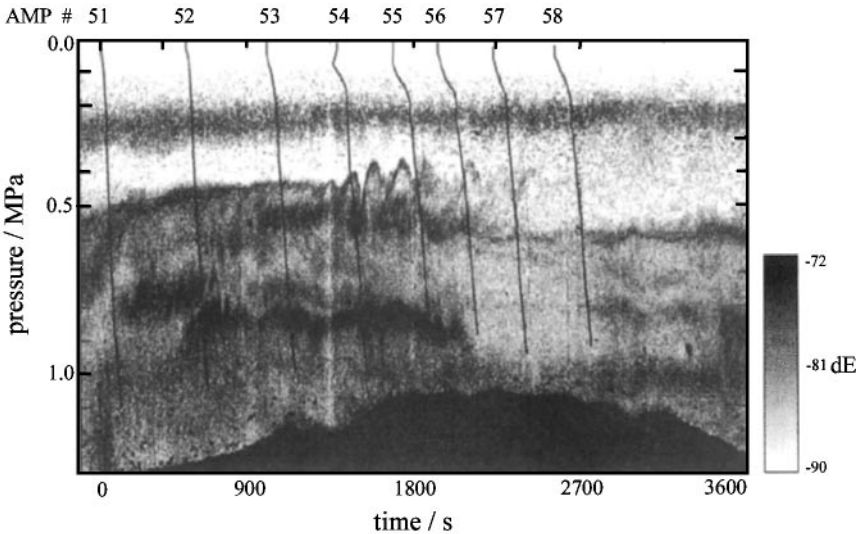

Figure 5 Kelvin-Helmholtz billows. An acoustic image showing pressure versus time of the acoustic scattering strength (1 MPa ≈ 100 m). The black lines mark trajectories of a free-fall microstructure probe (AMP) used to sample turbulence in and around the billows. (From Seim et al. 1995.)

first, which assumes that density and heat are mixed in the same way, is

$$K_v = \kappa C, \tag{1}$$

where C is the Cox number, $\langle (dT/dx)^2 \rangle / (dT_m/dz)^2$, measuring the variance of the temperature gradient $\langle (dT/dx)^2 \rangle$ (averaged over all three coordinate directions, but often, assuming isotropy, estimated in only one) divided by the square of the mean temperature gradient dT_m/dz (Osborn & Cox 1972). In principle, this allows K_v to be estimated from free-fall instruments measuring ocean temperature microstructure at subcentimeter scales.[4] The second is

$$K_\rho = \Gamma \varepsilon / N^2, \tag{2}$$

(Osborn 1980),[5] where the efficiency factor, Γ, is approximately 0.2 and N is the mean buoyancy frequency given by $N^2 = [g(d\rho_m/dz)/\rho_m]$, where ρ_m is the mean density at depth z and g is the gravitational acceleration. (The buoyancy frequency,

[4]A related parameter often referred to in the microstructure literature is the rate of loss of temperature variance, $\chi_T = 2\kappa_T \langle (dT/dx)^2 \rangle$, with the average, $\langle (dT/dx)^2 \rangle$, taken over all three directions, but frequently equated to $3\langle (dT/dz)^2 \rangle$, measured using vertical or free-fall instruments, assuming isotropy (often an uncertain assumption).

[5]Often ε can be measured more accurately than $\langle (dT/dx)^2 \rangle$, and Equation 2 often proves the more practical than Equation 1 as a means of estimating turbulent diffusivity.

N, varies from approximately 10^{-4} s^{-1} in the abyssal ocean to approximately 10^{-2} s^{-1} in the seasonal thermocline.) Assuming that the diffusion coefficient of heat, K_v, is equal to that of density, K_ρ, Equation 2 relates diffusion to the turbulent dissipation rate, ε. (In principle, Equations 1 and 2 provide a further way of finding ε: $\varepsilon = N^2\kappa C/\Gamma$.) The mean vertical distance over which denser water is carried over lighter water by turbulent motion in the density stratified ocean, resulting in a water column that, locally, is unstably stratified or statically unstable, can be estimated from fine-scale measurements of temperature and salinity from a free-fall or slowly lowered conductivity temperature depth (CTD) probe. The distance or displacement scale, L_T, is related to ε through the third relation:

$$\varepsilon = c_1 L_T^2 N^3, \tag{3}$$

where c_1 is a constant, approximately 0.64 (Dillon 1982).

Using Munk's average value for K_v and mean values of N, Equation 2 allows estimates to be made of the total rate of energy needed to mix the deep ocean, approximately 2.1 TW (1 Terrawatt $= 10^{12}$ W) summed over the oceans. To put this value into perspective, the total dissipation of energy from the tides is 3.7 TW, approximately 2.5 ± 0.05 TW of which is lost by the semidiurnal or lunar M_2 tidal component. Approximately 2.6 TW of the total tidal dissipation is known to be in turbulence in the bottom boundary layers of the shallow seas on the continental shelves surrounding the deep ocean (see Section 5).

The estimates of diffusion made from free-fall microstructure data caused some surprise. It was concluded that K_v is typically about 10^{-5} m^2 s^{-1}, an order of magnitude less than derived by Munk! There was controversy about the accuracy and sampling efficiency of the microstructure measurements. Confirmation of their reliability came from measurements of the rate of vertical spread of a neutrally buoyant tracer, sulphur hexafluoride (SF_6), made over a period of 30 months by Ledwell et al. (1993, 1998) in the North Atlantic. This is an elegant and novel way to obtain a measure of diffusion, effectively integrating over long times and over the large horizontal areas across which the tracer had spread. The accuracy of Munk's original estimate was now itself in doubt.

By the mid-1990s, convincing evidence of enhanced mixing near the lateral boundaries of the oceans had been discovered. Ledwell and collaborators (e.g., see Ledwell & Hickey 1995) showed that tracers released in mid-water within deep-water ocean basins off the Californian coast are more rapidly mixed vertically upon coming into contact with the sloping sides of the basins. Toole et al. (1997) found enhanced vertical diffusion around the flanks of seamounts, with K_v values of $(1–5) \times 10^{-4}$ m^2 s^{-1}; although, interpolating measurements to the seamounts of the whole North Pacific, they concluded that "the present limited data set does not support the idea that boundary mixing sustains an effective basin-average diffusivity of 1×10^{-4} m^2 s^{-1} at mid-depth in the Pacific."

A possible explanation for the discrepancy between Munk's estimate and the observed values of K_v came from measurements by Polzin et al. (1997) in the deep Brazil Basin adjoining the mid-Atlantic Ridge. Over the smooth abyssal

plane, values of K_v are consistent with those of earlier microstructure observations, approximately 10^{-5} m^2 s^{-1}, but at heights up to some 500 m over the rough topography of the Ridge, much greater values are observed (Figure 6), exceeding those of Munk's average value; rough topography leads to enhanced mixing (Ledwell et al. 2000).

The observations contained a further clue, one that proved significant: The dissipation rates appeared to have a Spring-Neap tidal signal. How might the tides be involved? It has been known for some time that the flow of the tides over topographic irregularities can generate internal waves of tidal frequency that radiate away from the topography. Baines (1982) estimated the total tidal energy transferred to internal tides around the continental slopes of the World Ocean as 0.016 TW $\pm$ 50%, much too small to account for the 2.1 TW needed for the mixing. At the time, this appeared to quash any suggestion that tides contribute significantly to the mixing. But Baines' estimates took no account of the internal waves generated by tidal flows over oceanic ridges. This can be much greater than that at the continental slopes, largely because the tidal flow may be directed across a ridge rather than (as is commonly the case) almost parallel to the continental slopes. Munk & Wunsch (1998) concluded that some 50% of the energy required for deep-ocean mixing comes from the tidal flow over ridges being locally converted into internal tides that, in propagating from their source and promoting internal wave breaking, produce mixing. (Off-bottom turbulence occurring within a radiating beam of tidal internal wave energy is demonstrated by Lien & Gregg 2001) (see Figure 7). Further mixing energy probably comes from internal waves generated largely at or near the surface of the deep ocean, mainly in regions of strong wind forcing (Watanabe & Hibiya 2002), possibly with enhanced breaking when the internal waves encounter with topography. Nagasawa et al. (2000) show that the earlier microstructure observations in the North Pacific that found K_v of order 10^{-5} m^2 s^{-1} are in locations where relatively low dissipation is to be expected, missing the likely locations of high dissipation. Their model results indicate a very patchy distribution of dissipation rates in the abyssal ocean.

The present understanding of vertical diffusion in the deep ocean is that it is distributed very unevenly, with hot spots of enhanced turbulence associated with bottom topography, particularly ridges, and generally increased levels at latitudes where internal waves are strongly generated at the sea surface. But the study remains unfinished. Evidence of internal tidal waves radiating to distances of 1000 km from the chain of Hawaiian Islands (Ray & Mitchum 1996, Merrifield et al. 2001) prompted a concentrated study in that region, the Hawaiian Ocean Mixing Experiment (HOME). Already there is striking evidence of agreement between model predictions of the locations of mixing and the observations (see Merrifield & Holloway 2002), but Rudick et al. (2003) conclude that "... isolated ridges are important sinks for surface-tide energy and sites of elevated mixing, but cannot account for a global eddy diffusivity of 1×10^{-4} m^2 s^{-1}." This may be too conservative a view: Niwa & Hibiya (2001) predict much greater surface-tide transfer rates at sites in the western Pacific. Just how the internal tides lose their

energy has yet to be revealed (e.g., see Finnigan et al. 2002). The effectiveness of internal wave generation at or near the sea surface by wind or mixed layer turbulence (see Section 3), the transfer of energy from near-inertial or tidal internal waves to turbulence or other internal waves, and the possible role of groups of internal waves in mixing (Thorpe 1999, 2001) are not fully understood or quantified. Dissipation in regions of rough topography cannot presently be estimated precisely, although observations in such regions (e.g., canyons; see Kunze et al. 2002) are now providing interesting and pertinent quantitative data.

A further very important conclusion reached by Munk & Wunsch (1998) is that the flux of heat of about 2 PW from equator to pole associated with the meridional overturning circulation of the World Ocean depends critically on the relatively less energetic vertical mixing. This provides a vital link between turbulent mixing and ocean circulation, which has a very substantial role in climate change. However the geographical and seasonal distribution of K_v, or of the mean rates of turbulent dissipation, in the deep ocean cannot yet be determined to the precision desirable for predictive ocean circulation models, nor can possible feedback in conditions of climate change be fully assessed.

5. TURBULENCE IN REGIONS AFFECTED BY TOPOGRAPHY

The leading part played by the bottom boundary layers of shallow seas in tidal dissipation has already been mentioned. The first estimation of their importance was by Taylor (1919), but it was not until the development of electromagnetic current meters, able to sample two components of motion rapidly on small (0.1 m) length scales, that the first measurements of turbulence or, more precisely, turbulent stress in the layers became possible (Bowden & Fairbairn 1956). Observations by Lien & Sanford (2000) using a newly developed instrument to measure vorticity (Sanford et al. 1999) show that the structure of the boundary layer is similar to that in the atmospheric boundary layer, although the velocity fluctuations produced by surface waves often have their effect.

The present state-of-the-art instrument for measuring ε in the bottom boundary layer and the three-dimensional eddy structure of the turbulence within which dissipation occurs uses particle image velocimetry (PIV). This measures and maps the motion of tiny particles suspended in the water in both space and time (Doron et al. 2001). The method consists of obtaining pairs of images by producing double pulses of a light sheet at 1 Hz frequency from which particle displacements can be obtained to produce a velocity map of approximately 29×29 velocity vectors spanning an area of 20×20 cm. Dissipation is derived by a spectral method. The device has been deployed on a bottom-mounted rig, but one that can be remotely raised or lowered. Because it demands power and high data rates, at present the rig is connected to an anchored vessel by an umbilical cable containing an optical fiber through which light is carried to the submerged optical probe.

Much of the recent attention given to turbulence in shelf seas has been directed at improving the performance and verifying numerical models of the structure of tidal flows or in developing measurements and estimates of sediment transport (e.g., see Thorne & Hardcastle 1997) and the movement of marine organisms, rather than in refining estimates of the total tidal dissipation. An important discovery that revealed the connection between bottom-generated turbulence and large-scale features, which also led the way in numerous further studies, was made by Simpson & Hunter (1974; see also Simpson 1981). The location of fronts between well-mixed (unstratified) and density-stratified waters is determined by the critical value of a parameter proportional to the third power of the tidal current amplitude and inversely proportional to water depth. In shallow regions of relatively fast tidal flows, turbulence generated by shear stress on the bottom extends to the surface and results in mixing throughout the water column, preventing stratification. Where turbulence is relatively weak or water depth large, the input of solar heat produces stratification that prevents complete mixing, and here a thermocline is maintained. Measurements of turbulence using a Fast Light Yoyo (FLY) free-fall instrument in a variety of differing conditions, including mixed and stratified regions, have defined and more precisely quantified the processes involved (Simpson et al. 1996, 2000, 2002; Rippeth et al. 2001). Because turbulence is generated by the shear in the tidal currents, which have two maximum values per tidal cycle, the dissipation rate has a periodicity of half that of the tide (i.e., about 6.2 h for the M_2 tide). Turbulent kinetic energy diffuses upwards from its source in the bottom boundary layer, and consequently, the time at which the maximum dissipation, ε, occurs is later at greater heights off the seabed. In unstratified waters, the maximum dissipation at a height of 70 m occurs approximately 2 h after that near the seabed (Figure 8*a*), but it may exceed 4 h at a height of 40 m in stratified conditions. In a mixed region of the 50-m deep southern North Sea, Nimmo Smith et al. (1999) use acoustic and visual observations to show that bottom-generated turbulent eddies can reach the water surface and form boils like those often seen in rivers in flood (Figure 9). The tide-generated boils are of diameter comparable with the water depth, and they supplement the dispersion caused at the sea surface by other processes, such as Langmuir circulation (Section 3).

A region of particular interest because of the anthropogenic impacts mentioned in the Introduction is that affected by fresh water run-off from land, areas near river mouths or estuaries, where there are consequently substantial horizontal salinity and density gradients and current shear. During ebb flow, the bottom stress reduces the near-bed flow, and less dense fresh water coming from land is consequently carried over the deeper dense water, increasing the vertical density gradients that confine bed-generated turbulence to the lower half of the water column. The opposite happens in conditions of flood tide, when the denser off-shore water is carried toward shore and the vertical density gradient is reduced, and mixing is often evident throughout the water column (see Figure 8*b*). In extreme conditions, termed overstrained by Nepf & Geyer (1996), the process may lead to dense (off-shore) water being carried over light (near-shore) water, producing statically

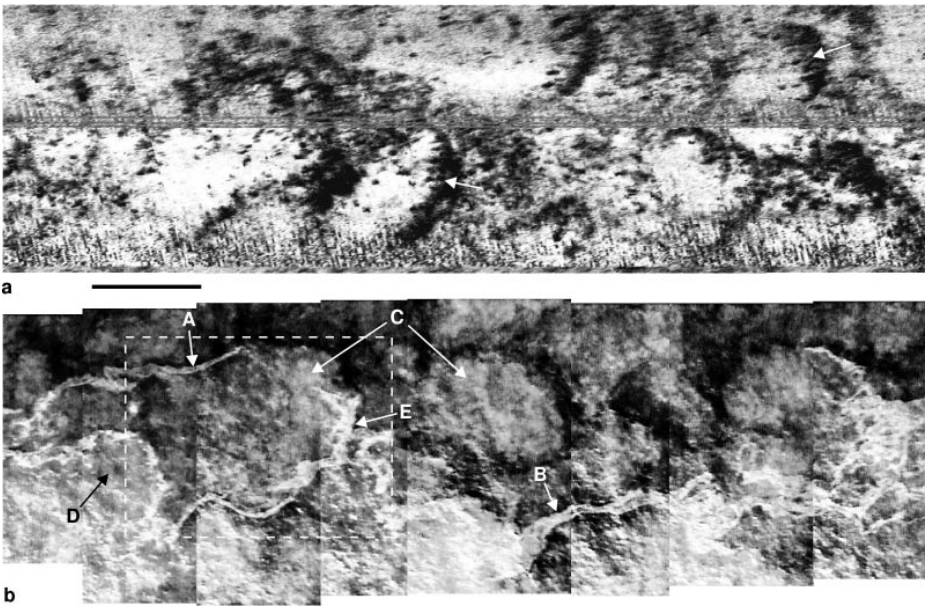

Figure 9 Surface manifestations of boils in a shallow tidal sea. The figure shows (*top*) an acoustic sidescan image of the sea surface taken from a seabed-mounted sonar. The near vertical bands at the bottom are caused by surface waves and (*bottom*) a composite video image of an oil slick (seen e.g., at *A* and *B*), but not coincident with the acoustic image. The scale bar is 50 m long, and the water depth is 45 m. The boils are the dark (high-scattering) near-circular features made visible in the acoustic image by enhanced wave breaking and bubble production, and in the visual image by holes in the oil film or by sediment (*C*). (From Nimmo Smith et al. 1999.)

unstable conditions in which convection supplements the turbulence generated at the sea bed.

Two indirect methods are now used to estimate ε remotely from on-board ship in surveys of coastal and shelf-sea areas. Each depends on Doppler sonar measurements. (Doppler sonar measures the shift in frequency of short pulses of sound reflected back to an emitter by particles suspended in the water, from which the speed of the water along the beam direction is determined.) Both methods stem from the idea that energy produced by the largest turbulent eddies cascades down to the small scales at which it is dissipated, and that the rate of energy production of turbulence is equal to the dissipation rate. In many cases, this is at least approximately so, although in stratified regions some leakage in the form of radiating internal waves will occur. Gargett (1999) argued and showed, by comparison with airfoil probe measurements, that dissipation is given by $\varepsilon = c_2 q^3/l$. Here, q is the rms vertical velocity component measured by a vertical Doppler sonar beam and l is a vertical scale (typically a few meters in the oceanic mixed layer) characteristic

of the large eddies and determined from the sonar measurements using a zero-crossing algorithm. The constant c_2 is approximately unity. The second method derived by Lohrmann et al. (1990; see also Lu & Lueck 1999) uses a more conventional acoustic Doppler current profiler (ADCP) to estimate the Reynolds stress and hence derive the rate of energy production.[6] Because of the beam geometry or presence of the vessel carrying ADCP, neither of these methods can be used to estimate ε very close to the sea surface.

Finally, two novel and cautionary sets of observations of flows confined by topography deserve mention. Both carry strong messages about the need for really comprehensive, model-testing observations and careful, critical modeling. Often, perhaps too often, it is assumed that flows are two-dimensional, in particular (but not only) when comparing theory and observations of flows in straits or over sills at the entrance to fjords. The assumption of two-dimensionality, usually made to simplify an analytical or numerical model, has so pervaded thinking that in planning observations there is sometimes little or no attempt to test whether the flow fields are really, or even approximately, two-dimensional. Often they are not. The observations by Klymak & Gregg (2001) of recirculating flows near the much-studied sill of Knight Inlet in British Columbia nicely reveals how such unexpected circulations may affect dissipation by transporting water from the turbulent lateral boundaries, influencing the development of stratified conditions and even changing the magnitude of the tidal flux. Further, it is often assumed that stratified flow through straits may be accurately described by inviscid (or zero Reynolds stress) theory in which the magnitude of the flow is controlled by a Froude number criteria, usually as the flow passes near the shallowest or narrowest part of the strait. This is well established and quite justified as a means to obtain insight into the magnitude of possible extreme flows. In reality, however, as these control points are approached, the flow is often modulated by the tides, with accompanying large shears or the steepening and breaking of internal waves. The consequent effects of turbulent transfers of momentum or buoyancy cannot be simply disregarded. That the actual flows may be strongly affected by turbulence is illustrated by surveys in the Bosphorus by Gregg et al. (1999). The measured composite critical internal Froude number, Fr (unity for an inviscid two-layer flow), is generally less than 0.2. This reduction of Fr is in accordance with the results of a numerical model devised by Winters & Seim (2000) that, appropriately, does include the effects of dissipation. Accounting for turbulence is essential for accurate prediction.

[6]The acoustic system has two pairs of beams. All the beams are inclined at approximately equal angles to the vertical (usually 20°–30°), the two pairs being at right angles. The correlation terms in the Reynolds stress, $-\rho\langle uw\rangle$, with horizontal and vertical velocity fluctuations, u and w respectively, and water density ρ, can be derived by differencing the square of the velocity components measured by a coplanar sonar pair (e.g., one beam pointing into the flow and the other in the direction in which the flow is going). The production rate is then given by $-\langle uw\rangle dU/dz$, where U is the mean horizontal flow at height z, determined by averaging the difference of the two velocity components.

6. CONCLUSION

The study of turbulence is one of great importance and current interest. Progress has come through the development of novel techniques and instruments reliable and sufficiently rugged to operate in the harsh ocean environment and when turbulence is most severe.

The connection between observations and models has been mentioned only briefly. It is impossible to represent the details of turbulent motion (or waves) within large-scale numerical models, and resort has to be made to representing the effects of turbulence, usually the flux it produces, in a parametric form in terms of quantities, such as currents and stratification, which are specifically represented and estimated in space and time within the model. In deriving a parametric representation, it is essential, however, to be aware of the processes that contribute most to turbulence and to be sure that the model itself responds to the quantities or measures on which these processes depend. Failure to include such measures within a model may be particularly dangerous in conditions of increased inputs from land or of changing climate when the relative importance of processes that determine ε, or even the probable location of turbulence, may also change.

The oceans are grossly undersampled and little is yet known of many of the processes that I have mentioned. Many more observations are essential if the modeling needed to address the pressing problems described in Section 1 is to be thoroughly tested and made sufficiently reliable for confident application.

ACKNOWLEDGMENT

I am grateful to those who have kindly given permission for figures to be reproduced.

The *Annual Review of Earth and Planetary Science* is online at http://earth.annualreviews.org

LITERATURE CITED

Agrawal YC, Terray EA, Donelan MA, Hwang PA, Williams III AJ, et al. 1992. Enhanced dissipation of kinetic energy beneath surface waves. *Nature* 359:219–20

Baines PG. 1982. On internal tidal generation models. *Deep Sea Res. A* 29:307–38

Baumeret H, Simpson J, Sündermann J, eds. 2004. *Marine Turbulence: Theories, Observations and Models*. Cambridge, UK: Cambridge Univ. Press. In press

Bowden KF, Fairbairn LA. 1956. Measurements of turbulent fluctuations Reynolds stresses in a tidal current. *Proc. R. Soc. London A* 237:422–38

Dewey RK, Crawford WR, Gargett AE, Oakey NS. 1987. A microstructure instrument for profiling oceanic turbulence in coastal bottom boundary layers. *J. Atmos. Ocean. Technol.* 4:288–97

Dillon TM. 1982. The mixing length of vertical overturns: a comparison of the Thorpe Ozmidov length scales. *J. Geophys. Res.* 87:9601–13

Doron P, Bertuccioli L, Katz J, Osborn TR.

2001. Turbulence characteristics dissipation estimates in the coastal ocean bottom boundary layer from PIV data. *J. Phys. Oceanogr.* 31:2108–34

Duncan JH. 1981. An investigation of breaking waves produced by a towed hydrofoil. *Proc. R. Soc. London A* 377:331–48

Finnigan TD, Luther DS, Lukas R. 2002. Observations of enhanced diapycnal mixing near the Hawaiian Ridge. *J. Phys. Oceanogr.* 32:2988–3002

Gargett AE. 1989. Ocean turbulence. *Annu. Rev. Fluid Mech.* 21:419–51

Gargett AE. 1999. Velcro measurements of turbulent kinetic energy dissipation rate, ε. *J. Atmos. Ocean. Technol.* 16:1973–93

Gemmrich JR, Farmer DM. 1999. Observations of the scale occurrence of breaking surface waves. *J. Phys. Oceanogr.* 29:2595–606

Gregg MC. 1999. Uncertainties limitations in measuring ε and χ_T. *J. Atmos. Ocean. Technol.* 16:1483–90

Gregg MC, Özsoy E, Latif MA. 1999. Quasi-steady exchange flow in the Bosphorus. *Geophys. Res. Lett.* 26:83–86

Gregg MC, D'Asaro EA, Shay TJ, Larson N. 1986. Observations of persistent mixing near-inertial internal waves. *J. Phys. Oceanogr.* 16:856–85

Jessop AT, Zappa CJ, Loewen MR, Hesany V. 1997. Infrared remote sensing of breaking waves. *Nature* 385:52–55

Jones IS, Toba Y. 2001. *Wind Stress Over the Ocean*. Cambridge, UK: Cambridge Univ. Press. 307 pp.

Kantha LH, Clayson CA. 2000a. *Numerical Models of Oceans Oceanographic Processes*. San Diego, CA: Academic. 940 pp.

Kantha LH, Clayson CA. 2000b. *Small Scale Processes in Geophysical Fluid Flows.* San Diego, CA: Academic. 888 pp.

Klymak JM, Gregg MC. 2001. Three-dimensional nature of flow near a sill. *J. Geophys. Res.* 106:22295–311

Kunze E, Rosenfield LK, Carter GS, Gregg MC. 2002. Internal waves in Monterey Canyon. *J. Phys. Oceanogr.* 32:1890–913

Langmuir I. 1938. Surface motion of water induced by wind. *Science* 87:119–23

Ledwell JR, Hickey BM. 1995. Evidence of enhanced boundary mixing in the Santa Monica Basin. *J. Geophys. Res.* 100:20665–79

Ledwell JR, Watson AJ, Laws CS. 1993. Evidence of slow mixing across the pycncline from an open-ocean tracer-release experiment. *Nature* 364:701–3

Ledwell JR, Watson AJ, Laws CS. 1998. Mixing of a tracer in the pycncline. *J. Geophys. Res.* 108:21499–529

Ledwell JR, Montgomery ET, Polzin KL, St Laurant LC, Schmitt RW, Toole JM. 2000. Evidence for enhanced mixing over rough topography in the abyssal ocean. *Nature* 403:179–82

Leibovich S. 1983. The form dynamics of Langmuir circulation. *Annu. Rev. Fluid Mech.* 198:391–427

Lien R-C, Gregg MC. 2001. Observations of turbulence in a tidal beam across a coastal ridge. *J. Geophys. Res.* 106:4575–91

Lien R-C, Sandford TB. 2000. Spectral characteristics of velocity vorticity fluxes in an unstratified turbulent boundary layer. *J. Geophys. Res.* 105:8659–72

Lohrmann A, Hacket B, Roed LP. 1990. High-resolution measurements of turbulence, velocity stress using a pulse-to-pulse coherent sonar. *J. Atmos. Ocean. Technol.* 7:19–37

Lu Y, Lueck RG. 1999. Using broadband ADCP in a tidal channel. Part II: turbulence. *J. Atmos. Ocean. Technol.* 14:1568–79

Lueck RG, Huang D, Newman D, Box J. 1997. Turbulence measurement with a moored instrument. *J. Atmos. Ocean. Technol.* 14:143–61

McWilliams JC, Sullivan PP, Moeng C-H. 1997. Langmuir turbulence in the ocean. *J. Fluid Mech.* 334:31–58

Melville WK, Matusov P. 2002. Distribution of breaking waves at the ocean surface. *Nature* 417:58–63

Melville WK, Veron F, White CJ. 2002. The velocity field under breaking waves: coherent structures turbulence. *J. Fluid Mech.* 454:203–33

Merrifield MA, Holloway PE. 2002. Model estimates of M2 internal tide energetics at the Hawaiian Ridge. *J. Geophys. Res.* 107:5-1–12, 107:10.1029/2001.JC000996

Merrifield MA, Holloway PE, Johnston TMS. 2001. The generation of internal tides at the Hawaiian Ridge. *Geophys. Res. Lett.* 28:559–62

Munk W. 1966. Abyssal recipes. *Deep Sea Res.* 13:207–30

Munk W, Wunsch C. 1998. Abyssal recipes II, energetics of tidal wind motion. *Deep Sea Res. 1* 45:1977–2010

Nagasawa M, Niwa Y, Hibiya T. 2000. Spatial temporal distributions of the wind-generated internal wave energy available for deep water mixing in the North Pacific. *J. Geophys. Res.* 105:13933–43

Nepf HM, Geyer WR. 1996. Intratidal variations in stratification mixing in the Hudson estuary. *J. Geophys. Res.* 101:12079–86

Nimmo Smith WAM, Thorpe SA, Graham A. 1999. Surface effects of bottom-generated turbulence in a shallow sea. *Nature* 400:251–54

Niwa Y, Hibiya T. 2001. Numerical study of the spatial distribution of the M_2 internal tide in the Pacific Ocean. *J. Geophys. Res.* 106:22441–49

Osborn TR. 1974. Vertical profiling of velocity microstructure. *J. Phys. Oceanogr.* 4:109–15

Osborn TR. 1980. Estimates of the local rate of vertical diffusion from dissipation measurements. *J. Phys. Oceanogr.* 10:83–89

Osborn TR, Cox CS. 1972. Oceanic fine structure. *Geophys. Fluid Dyn.* 3:321–45

Osborn TR, Farmer DM, Vagle S, Thorpe SA, Cure M. 1992. Measurements of bubble plumes turbulence from a submarine. *Atmos. Ocean* 30:419–40

Polzin KL, Toole JM, Ledwell JR, Schmitt RW. 1997. Spatial variability of turbulent mixing in the abyssal ocean. *Science* 276:93–96

Rapp RJ, Melville WK. 1990. Laboratory measurements of deep-water breaking waves. *Philos. Trans. R. Soc. London A* 331:735–800

Ray RD, Mitchum GT. 1996. Surface manifestations of internal tides generated near Hawaii. *Geophys. Res. Lett.* 23:2101–4

Rippeth TP, Fisher NR, Simpson JH. 2001. The cycle of turbulent dissipation in the presence of tidal straining. *J. Phys. Oceanogr.* 31:2458–71

Ruddick DL, Boyd TJ, Brainard RE, Carter GS, Egbert GD, et al. 2003. From tides to mixing along the Hawaiian Ridge. *Science* 301:355–57

Sanford TB, Carlson JA, Dunlap JH, Prater MD, Lien R-C. 1999. An electromagnetic vorticity velocity sensor for observing finescale kinetic fluctuations in the ocean. *J. Atmos. Ocean. Technol.* 16:1647–67

Schmitt RW, Toole JM, Koehler EC, Mellinger EC, Doherty KW. 1988. The development of a fine microstructure pofiler. *J. Atmos. Ocean. Technol.* 5:485–500

Seim HE, Gregg MC, Miyamoto RT. 1995. Acoustic backscatter from turbulent microstructure. *J. Atmos. Ocean. Technol.* 12: 367–80

Shay TJ, Gregg MC. 1986. Convectively driven turbulent mixing in the upper ocean. *J. Phys. Oceanogr.* 16:1777–98

Simpson JH. 1981. The shelf sea fronts: implications of their existence behaviour. *Philos. Trans. R. Soc. London A* 302:531–46

Simpson JH, Burchard H, Fisher NR, Rippeth TP. 2002. The semi-diurnal cycle of dissipation in a ROFI: model-measurement comparisons. *Cont. Shelf Res.* 22:1615–28

Simpson JH, Hunter JR. 1974. Fronts in the Irish Sea. *Nature* 250:404–6

Simpson JH, Crawford WR, Rippeth TP, Campbell AR, Choek JVS. 1996. The vertical structure of turbulent dissipation in shelf seas. *J. Phys. Oceanogr.* 26:1579–90

Simpson JH, Rippeth TP, Campbell AR. 2000. The phase lag of turbulent dissipation in tidal flow. In *Interactions Between Estuaries, Coastal Seas and Shelf Seas*, ed. TYanagi, pp. 57–67. Tokyo: Terra Sci. (TERRAPUB)

St Laurent L, Schmitt RW. 1999. The contribution of salt fingers to vertical mixing in the North Atlantic Tracer Release Experiment. *J. Phys. Oceanogr.* 29:1404–24

Staquet C, Sommeria J. 2002. Internal gravity waves: from instabilities to turbulence. *Annu. Rev. Fluid Mech.* 34:559–93

Stommel H. 1949. Trajectories of small bodies sinking slowly through convection cells. *J. Mar. Res.* 8:24–29

Taylor GI. 1919. Tidal friction in the Irish Sea. *Philos. Trans. R. Soc. London A* 220:1–93

Terray E, Donelan MA, Agarwal YC, Drennan WM, Kahma KK, et al. 1996. Estimates of kinetic energy dissipation under breaking waves. *J. Phys. Oceanogr.* 26:792–807

Thorne PD, Hardcastle PJ. 1997. Acoustic measurement of suspended sediments in turbulent currents comparison with *in-situ* samples. *J. Acoust. Soc. Am.* 101:2603–14

Thorpe SA. 1995. Dynamical processes of transfer at the sea surface. *Prog. Oceanog.* 35:315–52

Thorpe SA. 1998. Turbulence in the stratified rotating World Ocean. *Theoret. Comput. Fluid Dyn.* 11:171–81

Thorpe SA. 1999. On internal wave groups. *J. Phys. Oceanogr.* 29:1085–95

Thorpe SA. 2001. On the reflection of internal wave groups from sloping topography. *J. Phys. Oceanogr.* 31:3121–26

Thorpe SA. 2004. Langmuir circulation. *Annu. Rev. Fluid Mech.* 36:55–79

Thorpe SA, Nimmo Smith WAM, Thurnherr AM, Walters NJ. 1999. Patterns in foam. *Weather* 54:27–334

Thorpe SA, Osborn TR, Farmer DM, Vagel S. 2003b. Bubble clouds Langmuir circulation; observations and models. *J. Phys. Oceanogr.* 33:2013–31

Thorpe SA, Osborn TR, Jackson JFE, Hall AJ, Lueck RG. 2003a. Measurements of turbulence in the upper ocean mixing layer using Autosub. *J. Phys. Oceanogr.* 33:122–45

Toole JM, Polzin KL, Schmitt RW. 1994. Estimates of diapycnal mixing in the abyssal ocean. *Science* 264:1120–23

Toole JM, Schmitt RW, Polzin KL. 1997. Near-boundary mixing above the flanks of a midlatitude seamount. *J. Geophys. Res.* 102:947–49

Watanabe M, Hibiya T. 2002. Global estimates of the wind-induced energy flux to inertial motions in the surface mixed layer. *Geophys. Res. Lett.* 29:80-1–4, 29:10.1029/2001GL014422

Winters KB, Seim HE. 2000. The role of dissipation mixing in exchange flow through a contracting channel. *J. Fluid Mech.* 407:265–90

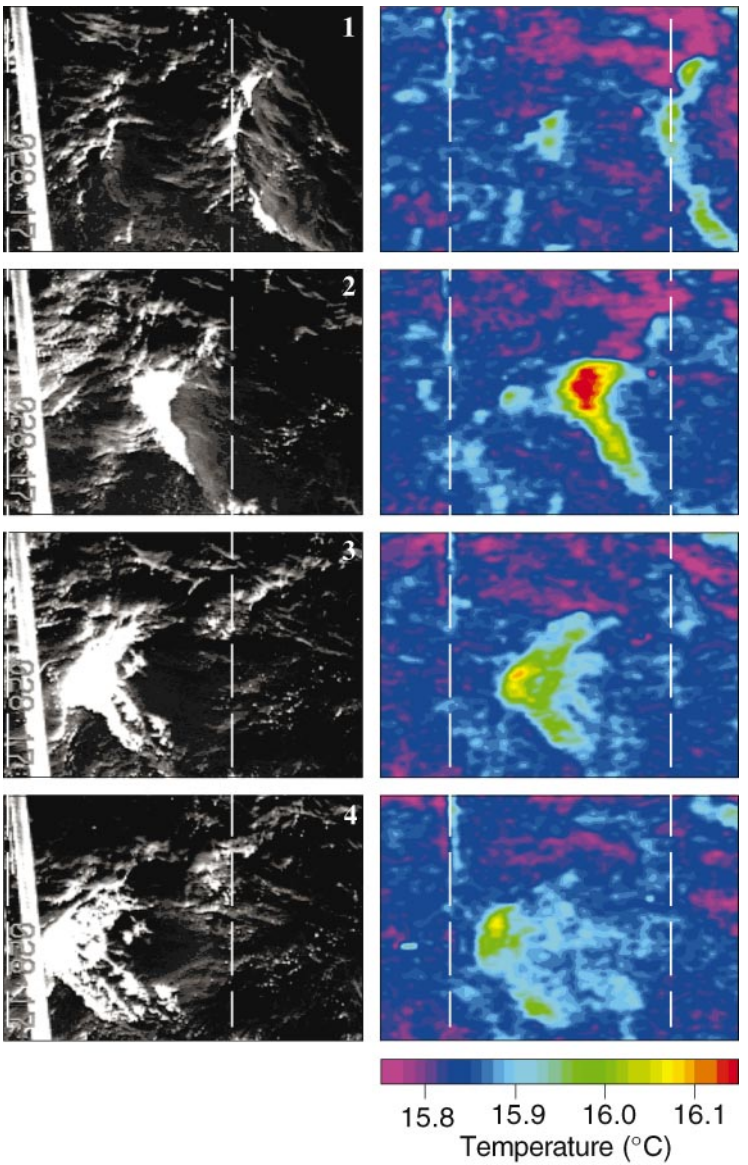

Figure 3 Surface temperature changes caused by a breaker. Sequence of simultaneous video (*left*) and infrared (*right*) images of a breaking wave in the open ocean spanning a period of 1.6 s. The image size is approximately 5 m $\times$ 10 m, and the breaking wave propagates to the left. The whitecap is the warmest region and leaves a roughly circular patch of warmer water. Wind speed 7.7 ms^{-1}. (From Jessop et al. 1997.)

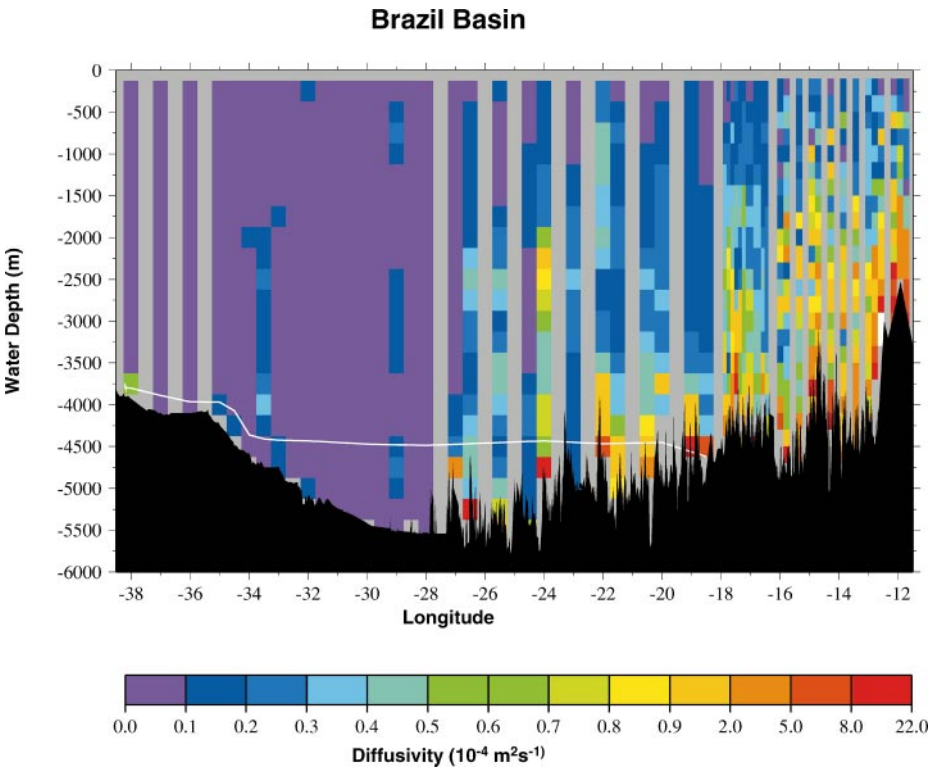

Figure 6 Vertical diffusivity in the Brazil Basin. A section of diffusivity estimated from measurements of turbulence in the deep ocean. Enhanced diffusivity is found over the rough topography of the mid-Atlantic Ridge to the right, with values exceeding 20 times Munk's basin-scale average. (From Polzin et al. 1997. Reprinted with permission of the American Association for the Advancement of Science.)

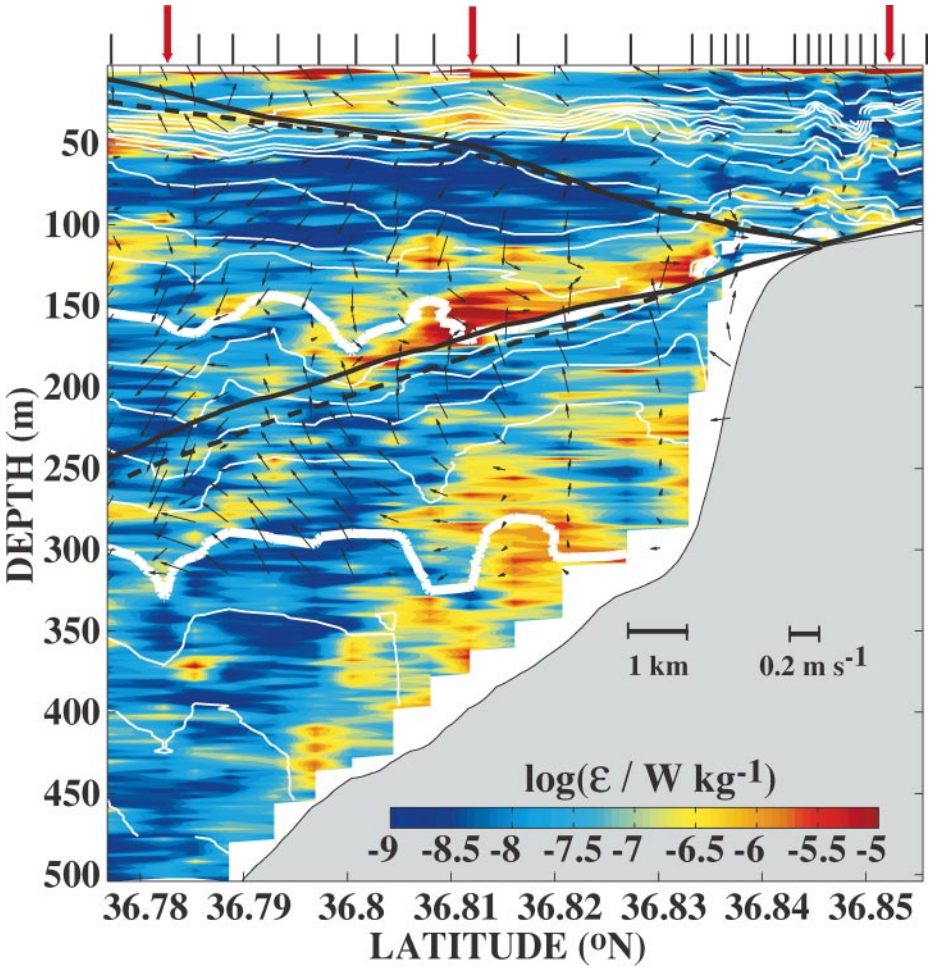

Figure 7 The enhancement of turbulent dissipation, ε, in an internal wave beam of tidal frequency propagating into deeper water in a region near the shelf break in Monterey Bay, California. The black lines mark the calculated location of beams of internal tides originating at the shelf break. (A dissipation of 1 Wkg^{-1} is the same as a rate of 1 $m^2\ s^{-3}$.) (From Lien & Gregg 2001.)

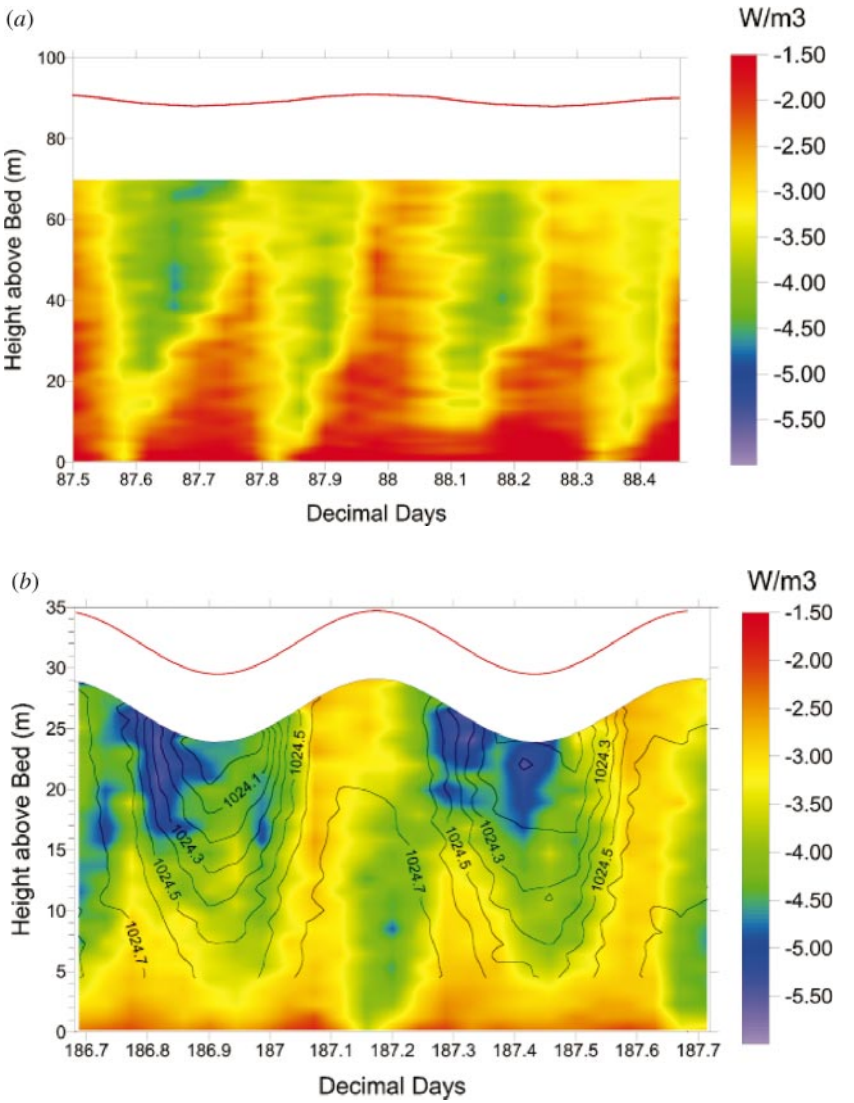

Figure 8 Turbulence in shallow seas. (*a*) A period of two M_2 tidal cycles showing the half-M_2 tidal period (6.2 h) variation of ε above the seabed in stratified shelf-sea waters. Greater values are found near the bottom and there is a time lag in ε as height above the bottom increases. (From Simpson et al. 2000.) (*b*) The variation of density (*lines*) and dissipation, ε (*colors*), made by a FLY microstructure instrument in a region of freshwater influence (ROFI). The strong turbulence is confined to the bottom 15 m during ebb (water depth shown at top decreasing), but extends throughout the water column during flood. [Units are $\log_{10}(\varepsilon; \mathrm{Wm^{-3}})$; a dissipation of 1 $\mathrm{Wm^{-3}}$ is the same as a rate of 1 $\mathrm{m^2 s^{-3}}$.] (From Simpson et al. 2002.) The upper red lines show the position of the sea surface.